Equation of state of stishovite and interpretation of SiO$_2$ shock-compression data

Wendy R. Panero

Department of Geological Sciences, University of Michigan, Ann Arbor, Michigan, USA

Laura Robin Benedetti

Department of Physics, University of California, Berkeley, California, USA

Raymond Jeanloz

Department of Earth and Planetary Science, University of California, Berkeley, California, USA

[1]   We present an isothermal equation of state for the high-pressure stishovite phase of SiO$_2$ based on synchrotron X-ray diffraction at 300 K to 60 GPa. The inferred equation of state is the same for stishovite synthesized from pure SiO$_2$ glass as from a natural, basalt glass that forms stishovite in association with other mineral phases, yielding a zero-pressure bulk modulus $K_{0T} = 312.9(\pm3.4)$ GPa and pressure derivative $K_0' = 4.8(\pm0.2)$. Our measurements of stishovite at static, high pressures predict a shock-compressed (Hugoniot) state that is 2.4 ($\pm$1.6)% denser than observed for SiO$_2$, suggesting that an amorphous phase, rather than stishovite, is produced under impact loading.   *INDEX TERMS:* 3919 Mineral Physics: Equations of state; 3924 Mineral Physics: High-pressure behavior; 3944 Mineral Physics: Shock wave experiments; 3954 Mineral Physics: X-ray, neutron, and electron spectroscopy and diffraction; *KEYWORDS:* high-pressure, silica, equations of state, Hugoniot, phase transitions

Citation: Panero, W. R., L. R. Benedetti, and R. Jeanloz, Equation of state of stishovite and interpretation of SiO$_2$ shock-compression data, *J. Geophys. Res.*, *108*(B1), 2015, doi:10.1029/2001JB001663, 2003.

1. Introduction

[2]   The high-pressure silicate phases deep inside the Earth and other large terrestrial planets are characterized by silicon in octahedral coordination with oxygen. Stishovite, the first such phase to be identified, is the rutile-structured form of SiO$_2$ stable between 7 and 54 GPa [*Stishov*, 1964; *Andrault et al.*, 1998; *Hemley et al.*, 2000]. After its discovery in the laboratory under static conditions, it was identified in Meteor Crater and became an indicator of natural impact-induced shock-wave processes [*Chao et al.*, 1962; *Kieffer*, 1971; *Kieffer et al.*, 1976; *Sharp et al.*, 1999]. The properties of stishovite at high pressures have been of long-standing interest, especially in geophysics, planetary science, and crystal physics [*Wackerle*, 1962; *Al'tshuler et al.*, 1965; *Podurets et al.*, 1976; *Marsh*, 1980; *Jackson and Niesler*, 1982; *Lyzenga et al.*, 1983; *Furnish and Ito*, 1996].

[3]   Measurements of its equation of state have been challenging, however, both due to its high bulk modulus and due to the difficulty in obtaining adequate samples [*Hemley et al.*, 2000; *Liu et al.*, 1974; *Li et al.*, 1996; *Ross et al.*, 1990; *Sugiyama et al.*, 1987; *Sato*, 1977a, 1977b; *Olinger*, 1976; *Ahrens et al.*, 1969]. Therefore, it has been studied extensively under static as well as dynamic compression. Because of sample-size requirements, the starting material for shock-wave experiments is generally a low-pressure phase of SiO$_2$ (e.g., crystalline quartz or amorphous silica), and it is then assumed that the thermodynamically stable, high-pressure stishovite phase is formed under shock conditions [e.g., *Wackerle*, 1962; *Lyzenga et al.*, 1983; *Ahrens et al.*, 1969; *McQueen et al.*, 1963]. Here we provide room temperature and static-compression measurements that allow a critical assessment of the state achieved under dynamic loading along the shock-compression Hugoniot of SiO$_2$ at pressures of $\sim$10–100 GPa. Such an analysis requires a model for the equation of state both under isothermal conditions and under shock loading. The mutual compatibility of these models has been shown for other materials, such as MgO [*Jackson and Niesler*, 1982].

[4]   Comparisons of the elastic properties of (end-member) pure phases to the varying compositions found in natural samples are crucial for evaluating the reliability of geophysical interpretations based on laboratory measurements. While measurements made on a single-phase system are simpler and more direct, experiments have shown that the incorporation of minor elements into materials can have unpredictable effects. For instance, the incorporation of iron into MgSiO$_3$-perovskite does not appear to affect the compressibility of the material despite expanding the lattice [*Mao et al.*, 1991]. Aluminum, however, appears to distort as well as expand the lattice, leading to measurable changes in the compressibility [*Kubo and Akaogi*, 2000; *Zhang and Weidner*, 1999; *O'Niell and Jeanloz*, 1994]. In contrast to its behavior in perovskite, iron in MgO has been shown to have

Table 1. Composition of Starting Materials

Basalt Glass, wt.%		Suprasil 2, ppm	
SiO_2	50.6	Al	0.1
Al_2O_3	13.6	Ca	0.1
FeO	12.5	Fe	0.2
MgO	6.5	Mg	0–0.1
CaO	11.1		
H_2O	0.2	H_2O	<1000

a significant effect on compressibility as well as lattice parameters. To our knowledge, no direct comparisons have been previously made between the compression observed for stishovite formed from pure SiO_2 and from a natural rock.

2. Experimental Methods and Results

[5] Samples were compressed to static high pressures in a diamond-anvil cell, and laser heated in situ to produce stishovite, at pressures between 17 and 60 GPa and temperatures in excess of 2000 K. Experiments were performed with a Mao-Bell cell [*Mao et al.*, 1979] or a symmetrical diamond cell [*Mao and Hemley*, 1998], using 350 μm culets and spring-steel gasketting material. A typical sample diameter under pressure was 150 μm. A 20-W cw Nd:YAG or a YLF laser was used to heat the sample. High-temperature synthesis and annealing reduces nonhydrostatic stresses, allowing a reliable, hydrostatic equation of state to be determined for stishovite without the use of a fluid pressure medium [*Andrault et al.*, 1998; *Knittle and Jeanloz*, 1987]. We used two starting materials: (1) a sample of pure fused silica intermixed with 9.2 wt.% Pt, and (2) a natural volcanic glass (MORB) that forms 10–20 vol.% stishovite at high pressures [*Irifune and Ringwood*, 1993; *Funamori et al.*, 2000]. Compositions are listed in Table 1. These compositions provide direct comparisons between the equations of state of high-pressure phases formed from synthetic versus natural materials.

[6] Room temperature measurements of unit-cell volumes were obtained by synchrotron X-ray diffraction after laser heating, both at high pressure and upon decompression. Angular dispersive X-ray diffraction patterns of the pure silica samples were collected onto image plates at SSRL beamline 10–2. Energy dispersive X-ray diffraction data were collected on the MORB composition at APS GSECARS beamline 13-IDD. Volumes were determined by using the [110], [111], [210], [121], and [220] diffraction lines of stishovite. Pressures (P) were determined by a

combination of ruby-fluorescence [*Mao et al.*, 1978] and volume measurements of internal standards (MgO or Pt) (Table 2) [*Jackson and Niesler*, 1982; *Holmes et al.*, 1989], where pressure uncertainties were propagated from the uncertainties in the standards' equations of state. Consistency among multiple pressure standards, using different calibration methods and obtaining pressures from several ruby grains per sample, provides experimental evidence for pressures being essentially hydrostatic after heating (Table 2). A transition to the $CaCl_2$ phase is expected at about 55–60 GPa [*Andrault et al.*, 1998] but was not observed in the present study. This could be due to the fact that the transition was not reached in these experiments (no splitting seen in the [121] line), or due to overlapping diffraction lines of the internal standard obscuring the small splitting of the stishovite [120] line indicative of the transition. Indeed, the transition pressure appears to vary between experiments [48–100 GPa; *Hemley et al.*, 2000; *Tsuchida and Yagi*, 1989], which may indicate that it is a strain-driven transition. Nevertheless, the unit-cell volumes determined in the present study are indistinguishable from those of previous quasi-hydrostatic [*Hemley et al.*, 2000] and hydrostatic [*Ross et al.*, 1990] single-crystal diffraction measurements up to 36 GPa (Figure 1). In order to avoid potential systematic errors, volumes are referenced to the zero-pressure values obtained in each study; high-pressure volumes and uncertainties are listed in Table 2.

3. Analysis of Static-Compression Data

[7] As demonstrated by *Birch* [1978], the normalized pressure, F, provides a sensitive means of analyzing finite-compression data, where

$$F = \frac{P}{3f(1 + 2f)^{5/2}} \quad (1)$$

is a function of the Eulerian strain

$$f = \left[(v/v_0)^{-2/3} - 1 \right]/2 \quad (2)$$

where P is the pressure, v is the pressure-dependent unit-cell volume, and v_0 refers to the value at zero pressure. A Taylor expansion of the free energy as a function of f yields the finite-strain equation of state [*Birch*, 1978]

$$P = 3f(1 + 2f)^{5/2}K_{0T}\left[1 + 1.5\left(K'_{0T} - 4\right)f + \ldots\right] \quad (3)$$

Table 2. Isothermal Compression Data for Stishovite (SiO_2)

| Pressure, GPa	v, Å^3	v/v_0	Starting Material	Synthesis/Decompression	Pressure Standard
59.2 (1.6)	40.50 (1)	0.873 (1)	MORB glass	S	Ruby
56.0 (2.4)	40.29 (2)	0.878 (1)	Fused silica	S	Ruby/Pt
46.9 (1.4)	41.67 (1)	0.892(3)	MORB glass	S	Ruby
43.2 (1.1)	42.115(6)	0.8988 (4)	MORB glass	S	MgO
35.2 (0.8)	43.02 (2)	0.914 (1)	MORB glass	D	MgO
29.9 (0.3)	43.00 (1)	0.9238 (8)	Fused silica	D	Pt
26.0 (1.0)	43.83 (2)	0.932 (1)	MORB glass	S	MgO
17.6 (0.5)	44.56 (2)	0.951 (2)	MORB glass	D	Ruby
2.45 (0.2)	46.10 (1)	0.9924 (3)	Fused silica	D	Pt
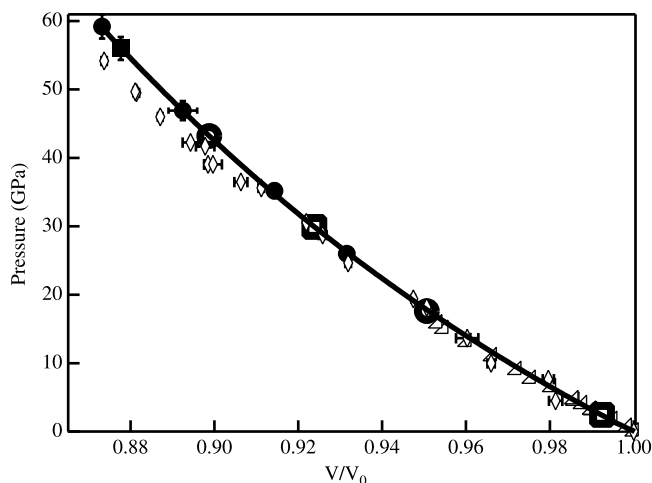
Figure 1. *P-v* data for stishovite, with volumes normalized to the zero-pressure value (v_0) measured for each sample. Squares and circles are for stishovite synthesized from fused silica and MORB, respectively; closed and open symbols indicate points taken on synthesis and decompression, respectively. Triangles are from the work of *Ross et al.* [1990], and diamonds from the work of *Hemley et al.* [2000].

with the bulk modulus K_{0T} and pressure derivative K'_0 being determined by the intercept and slope of data plotted as F versus f by applying equation (1) to equation (3)

$$F = K_{0T}\left[1 + 1.5\left(K'_{0T} - 4\right)f + \ldots\right] \qquad (4)$$

Thus the data from Table 2 (Figure 1; P versus v/v_0) can be recast in terms of equations (1) and (2) as in Figure 2 in order to make a direct comparison of finite-compression data with wave-velocity (e.g., Brillouin-scattering) measurements.

[8] A linear fit to our compression measurements as F versus f, corresponding to a third-order Birch-Murnaghan equations of state (3) and (4) [*Birch*, 1978], yields $K_{0T} = 311.4(\pm6.7)$ GPa, $K'_0 = 4.9(\pm0.4)$, in excellent agreement with the independent Brillouin measurements of $K_{0T} = 313.4(\pm4.0)$ GPa [*Weidner et al.*, 1982] (recalculated from the adiabatic value $K_{0S} = 316.0(\pm4.0)$ GPa using data in Table 4). This consistency argues for our measurements describing the stishovite hydrostatic equation of state, in accord with the experimental evidence cited above for effective hydrostatic conditions being commonly achieved upon laser heating inside the diamond cell. Including the zero-strain (Brillouin-scattering) value with our data yields $K_{0T} = 312.9(\pm3.4)$ GPa and $K'_0 = 4.8(\pm0.2)(\chi^2 = 0.89)$. The measurements also confirm that stishovite formed in natural MORB exhibits elastic compression indistinguishable from pure stishovite created from high-quality synthetic silica (Figures 1 and 2). Analytical transmission electron microscopy (ATEM) measurements of the compositions of stishovite formed in similar samples [*Funamori et al.*, 2000; *Kesson et al.*, 1994] show a small amount of Al incorporation into the silica phase, but the technique and small-grain size imply large uncertainties. No significant, systematic differences were found in the v_0 measurements between the pure stishovite and that formed in MORB ($\Delta v_0/v_0 = 0.2 \pm 0.5\%$). Fitting the data sets for the different starting materials

independently gives $K_{0T} = 313.6(\pm8.7)$ GPa and $K'_0 = 4.8(\pm0.6)$ for the fused silica starting material and $K_{0T} = 308.0(\pm10.6)$ GPa and $K'_0 = 5.1(\pm1.1)$ GPa for the basalt. These results are summarized in Table 3.

[9] A strong correlation between K_{0T} and K'_0 (slope and intercept on Figure 2) exists in the independent as well as the combined fits. Figure 2b shows that for reasonable values of χ^2 (≤1), the equation of state can vary between $K_{0T} = 311$GPa, $K'_0 = 4.6$ and $K_{0T} = 315$GPa, $K'_0 = 5.0$ well within the uncertainties of these parameters from the best fit in Table 3.

[10] Though good at low pressures, agreement with the single-crystal results degrades above 36 GPa (Figures 1 and 2). We believe that this is due to systematic errors influencing the single-crystal data, for two reasons. First, the older
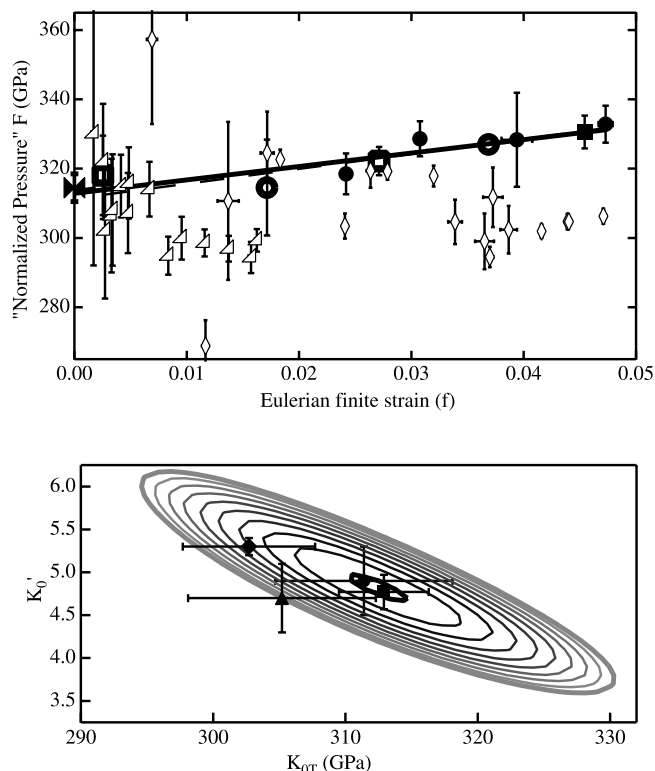

Figure 2. (a) Data as normalized pressure F versus Eulerian strain parameter f. Symbols are the same as in Figure 1, and the bow-tie shows the K_{0T} value obtained from Brillouin spectroscopy [*Weidner et al.*, 1982]. (b) Contour map of χ^2 showing the trade-off between K_{0T} and K'_0 for the present data set, and the statistical compatibility of three equations of state: a fit to our measurements alone (dashed line in Figure 2a, circle in Figure 2b); a fit to our data plus the Brillouin measurement (solid line in Figure 2a, square in Figure 2b); and a fit to the cumulative set of all static-compression data (triangle in Figure 2b: $K_{0T} = 305.2(\pm7.1)$ GPa, $K'_0 = 4.7(\pm0.4)$, $\chi^2 = 1.07$). For comparison, *Li et al.*'s [1996] high-pressure ultrasonics measurements are shown (diamond) indicating further consistency between measurements. Contours are lines of equal χ^2 for our data set, where the inner and outer lines are for $\chi^2 = 1$ and 10. Based on this statistical analysis, we choose $K_{0T} = 312.9(\pm3.4)$ GPa, $K'_0 = 4.8(\pm0.2)$ GPa as fit to our data plus the Brillouin measurement as the best value (Table 4).

Table 3. Summary of Equation of State Fits

Starting Material	K_{0T}, GPa	K_0'	Technique
MORB data	308.0 ± 10.6	5.1 ± 1.1	
Synthetic silica	313.6 ± 8.7	4.8 ± 0.6	
MORB + silica	311.4 ± 6.7	4.9 ± 0.4	
All data + Brillouin	312.9 ± 3.4	4.8 ± 0.2	
Hemley et al., 2000	298 ± 8	3.98 ± 0.46	Single x-stal; He pressure medium; $P < 65$ GPa
Ross et al., 1990	313 ± 4	1.6 ± 0.6	Single x-stal; 4:1 meth:eth; $P < 15$ GPa
Li et al., 1996	305 ± 5	5.3 ± 0.1	Ultrasonics, $P < 3$ GPa

measurements [*Ross et al.*, 1990] are incompatible, within quoted uncertainties, with the Brillouin-scattering and more recent single-crystal measurements [*Hemley et al.*, 2000] above 6–8 GPa (Figure 2). Second, the more recent single-crystal data exhibit a break in the compression curve (or its slope) at 36 GPa, even though there is no evidence of any structural transition until higher pressure (in fact, the structural distortion at 55–60 GPa appears not to involve a volume change [*Andrault et al.*, 1998; *Hemley et al.*, 2000]). Thus given the agreement between our finite-compression measurements and the zero-strain Brillouin data, we conclude that a simple equation of state defined by equation (3) and the parameters in Table 3 describes the room temperature compression of stishovite to 50–55 GPa.

[11] A significant finding is that the value of K_0' for stishovite is close to 5, higher than for most crystals but well in line with results that have been obtained for other rutile-structured oxides [e.g., *Sato*, 1977a, 1977b]. Our measurements thus reinforce *Li et al.*'s [1996] conclusion that the bulk-modulus pressure derivative of stishovite is high, the coupled values of $K_{0T} = 302.7(\pm5)$ GPa and $K_0' = 5.3(\pm0.1)$ obtained from their study being compatible (within 1–2 estimated standard deviations) with our results (Figure 2b).

4. Comparison With Shock-Wave Measurements

[12] Shock compression of silica to pressures above 15–20 GPa produces small amounts (<1 vol.%) of stishovite, both in nature [*Chao et al.*, 1962; *Kieffer*, 1971; *Kieffer et al.*, 1976] and in the laboratory [*DeCarli and Milton*, 1965; *Schneider and Ashworth*, 1985]. Although the shock-wave equation of state of SiO_2 traditionally has been used to infer the properties of stishovite at high pressures [*Wackerle*, 1962; *Al'tshuler et al.*, 1965; *Marsh*, 1980; *Ahrens et al.*, 1969; *McQueen et al.*, 1963], debate remains as to whether stishovite truly represents the bulk of the state of SiO_2 achieved dynamically under shock loading [*Kieffer et al.*, 1976; *Kondo et al.*, 1983]. This can be addressed by comparing shock-Hugoniot measurements on silica with the equation of state that we have determined for stishovite. Using Table 4 and a Mie-Grüneisen equation of state based on equation (3), the experimental measurements of shock-wave (U_S) and particle (u_p) velocities,

$$U_S = V_0 \left[\frac{P_H}{V_0 - V_H} \right]^{1/2} \quad (5)$$

$$u_p = [P_H(V_0 - V_H)]^{1/2} \quad (6)$$

provide for the determination of Hugoniot pressure (P_H) at a particular specific volume (V_H) through conservation of mass, momentum, and energy across the shock front:

$$P_H = \frac{\left[P_S + \frac{\gamma}{V_H} \left(\int_{V_{02}}^{V_H} P_S dV - E_{tr} \right) \right]}{1 - \frac{\gamma}{V_H} \left(\frac{V_{01} - V_H}{2} \right)} \quad (7)$$

where γ and P_S are the Grüneisen parameter and isentrope pressure of the high-pressure phase at V_H, and the internal energy of transition $E_{tr} = E_{02} - E_{01}$ subscripts 01 and 02 indicate zero-pressure values for the initial (low pressure) and final (high pressure) phases, respectively. The isentrope pressure P_S is determined using equation (3) by substituting K_{0S} for K_{0T}'; previous work has shown the compatibility between the Birch-Murnaghan and the Mie-Grüneisen equations of state [*Jackson and Niesler*, 1982; *Birch*, 1978]. In the case of MgO, for example, *Jackson and Niesler* [1982] find a density difference of less than 0.5% throughout a range of over 40% compression, well within the range of the uncertainties of the data.

[13] In this way, we can predict the Hugoniot equations of state for stishovite formed from different initial phases, such as fused silica or crystalline quartz, and compare the predictions to published experimental results. Figure 3 shows the shock data as P_H versus V_H used in the analysis presented here. Consideration of more than one initial density (i.e., different starting materials) yields a broader
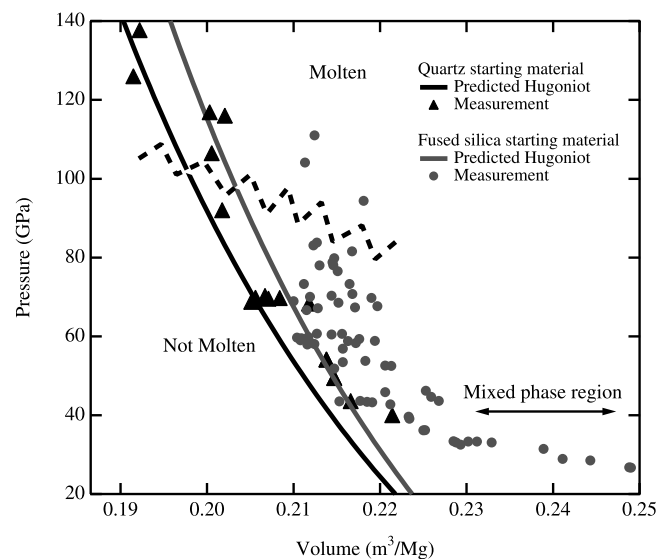

Figure 3. Shock pressure and volumes for fused silica (circles) and crystalline quartz (triangles) [*Marsh*, 1980; *Lyzenga et al.*, 1983] starting materials. Black line is the predicted Hugoniot for a crystalline quartz starting material, while the gray line is predicted for a fused silica starting material. The jagged line indicates the approximate melting conditions upon shock loading from the work of *Lyzenga et al.* [1983]. Below 40 GPa, the fused silica is still in a mixed phase region, not representative of the high-pressure phase. Measurements consistently lie at larger volumes (lower densities) than predicted.

Table 4. Thermodynamic Data Used in Hugoniot Models

Parameters	Values	References
γ	1.35[a]	Wanatabe [1982]
α	1.64×10^{-5}/K1	Ito et al. [1974]
K_{0T}	312.9 ($\pm$3.4)[a] GPa	
$K_{0S} = (1 + \alpha\gamma T)K_{0T}$	315.0 ($\pm$3.4)[a] GPa	
K_0'	4.8 ($\pm$0.2)[a]	
E_{tr} (quartz to stishovite)	8.9×10^5 J/kg	Robie [1968]
E_{tr} (fused silica to stishovite)	7.0×10^5 J/kg	Robie [1968]
$q = d\ln\gamma/d\ln v$	1[b]	
ρ_0 (fused silica)	2.204 g/cm^3	
ρ_0 (single-crystal quartz)	2.650 g/cm^3	
ρ_0 (stishovite)	4.287 g/cm^3	

[a]This study.
[b]Assumed.

range of final states, because a lower initial density results in a higher Hugoniot pressure (due to higher temperature) at a particular final volume V_H. Data at pressures below about 40 GPa reflect a mixed-phase region in which the transformation to the high-pressure form is incomplete. These data are neglected in the analysis presented here, but are shown to indicate the number of Hugoniot measurements that have been collected on SiO$_2$.

[14] A close analysis shows that Hugoniot measurements [*Marsh*, 1980; *Lyzenga et al.*, 1983] are systematically lower in particle velocity, for a given shock-wave velocity, than is expected for stishovite (Figure 4). This is true for either starting material, and means that the Hugoniot state has a 2.4% larger volume than expected for stishovite (see equation (6) and Figure 3). The density deficit is systematic, and lies well outside the estimated error bound of 1.6% (Figure 4b). This calculation of the stishovite Hugoniot is most sensitive to the isothermal equation of state and the Grüneisen parameter. A significantly stiffer equation of state will decrease the discrepancy between the calculated Hugoniot and the measured shock data. To match the measured data, the isothermal bulk modulus would have to exceed 340 GPa, 8σ greater than constrained by the data. Moreover, should our interpretation of the static-compression data be incorrect, and a lower, more typical value of K_0' ($\sim$4) be more appropriate for the equation of state of stishovite (shallower slope in Figure 2), the discrepancy with respect to the Hugoniot data summarized in Figure 3 is increased. Thermodynamically based Grüneisen parameter determinations for stishovite vary between 1.3 and 1.5 [*Robie*, 1968; *Swamy et al.*, 1994] while the average mode Grüneisen parameter tends to be much lower, about 0.85 [*Williams et al.*, 1993]. A lower γ predicts a significantly more dense Hugoniot (due to lower shock temperatures). Therefore using the more accurate, thermodynamically based Grüneisen parameter, will also predict a hotter, and therefore less dense Hugoniot. Further, varying q (=$d\ln\gamma/d\ln v$) between 0.5 and 2.0 (cf. Table 4) does not change these results but it does change the slope of the predicted U_s-u_p relationship, thereby inducing a slope in the error envelope for the density residuals (Figure 4b). As the difference between predicted and observed Hugoniot densities does not vary systematically with pressure (within mutual uncertainties), the assumed value of $q = 1$ is the best that can be presently adopted. Therefore we conclude that stishovite is not the primary state formed along the Hugoniot of quartz or fused silica at 40–80 GPa.

[15] While data exist on the shock compression of coesite [*Podurets et al.*, 1976] and stishovite [*Furnish and Ito*, 1996], they are sparse and have varying initial densities, with little indication of the uncertainties in the measurements. This makes it difficult to produce a quantitative comparison with the current calculation of the Hugoniot. Though inconclusive, these measurements do indicate that the shock data for coesite as a starting material also produces Hugoniot states less dense than predicted here for stishovite.

[16] Shock-temperature measurements indicate that SiO$_2$ melts upon shock compression at pressures above 80–100 GPa (particle velocity exceeding 4.4 km/s) [*Lyzenga et al.*, 1983]. The density of liquid silica determined by shock compression is lower than that of crystalline SiO$_2$, in either the stishovite (from our measurements) or the CaCl$_2$ structure [from the work of *Andrault et al.*, 1998 and *Hemley et*
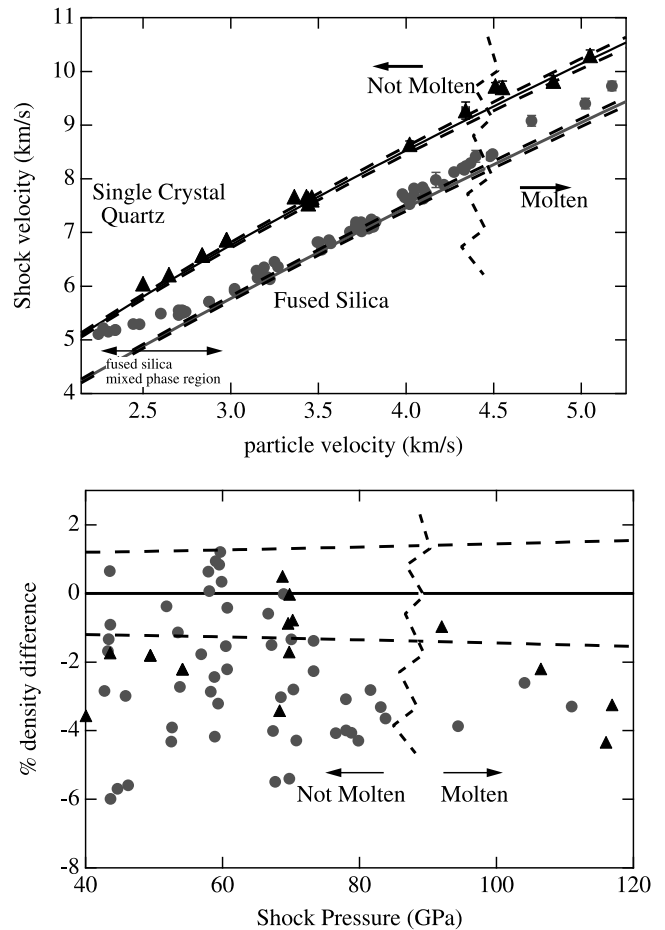

Figure 4. (a) Shock velocity-particle velocity (U_S-u_p) relationship predicted for stishovite from our isothermal equation of state (Table 4), for fused silica (dashed) and crystalline quartz (solid) starting materials. Symbols are as in Figure 3, and dotted lines indicate the uncertainties in the calculated equations of state. (b) Percent density difference between the available Hugoniot data and the model predicted by the present equation of state for stishovite, showing that the shock data consistently yield lower densities than predicted.

al., 2000], by about 4 (±2)% at 80–100 GPa. Thus the density difference between the crystalline stishovite (calculated) and liquid silica (measured) implies a positive Clapeyron slope, $dT_m/dP = \Delta V/\Delta S$ (positive changes in volume and entropy from the solid to the liquid state) for the melting temperature T_m of SiO_2 over this pressure range.

[17] The Hugoniot of SiO_2 appears to be continuous at 70–90 GPa, with no resolvable density change across the melting transition (Figure 4b). The similarity of volumes for the molten and solid portions of the Hugoniot suggests that shock-compressed SiO_2 may be in an amorphous state, rather than crystalline stishovite, at pressures of 50–80 GPa. Crystalline SiO_2 becomes amorphous upon compression under kinetically hindered conditions (e.g., low temperatures or short timescales [Hemley et al., 1988; Kingma et al., 1993]). Therefore our results support the inference that a dense amorphous state, rather than crystalline stishovite, forms in the shock-compressed state along the SiO_2 Hugoniot [Hemley et al., 2000; Kondo et al., 1983; Stöffler and Hornemann, 1972; Gratz et al., 1992; Ng et al., 1991].

[18] To elaborate, pressure induces the same coordination changes in the glass more readily (i.e., at lower temperatures and more rapidly) [Williams et al., 1993] than in crystalstructural transitions among the equilibrium silica polymorphs. Although, stishovite is found associated with impact structures in nature, detailed observations indicate that little stishovite is actually formed from the initial quartz grains, and then only along grain boundaries: regions out of equilibrium with the bulk material [Kieffer et al., 1976]. Shock-recovery experiments also return only trace amounts of stishovite, along with more abundant glass [DeCarli and Milton, 1965; Schneider and Ashworth, 1985; Stöffler and Hornemann, 1972; Gratz et al., 1992]. The retrieval in such experiments of limited amounts of stishovite along with a large amount of densified glass [DeCarli and Milton, 1965; Schneider and Ashworth, 1985] can thus be explained by the initially crystalline quartz amorphizing upon shock loading, with coordination changing readily in the amorphous state, along with trace amounts of stishovite forming at high pressure, before unloading yields a largely glassy material (with most of the octahedrally coordinated Si reverting to tetrahedral coordination on decompression [Williams et al., 1993]). An alternative is that the quartz of fused silica transforms to a metastable phase, either Fe_2N [Liu et al., 1978] or $P2_1/c$ structure [Haines et al., 2001]. However, due to a lack of a distinct lack of a break in the Hugoniot upon melting, these structures are less likely than a primarily amorphous phase.

[19] In conclusion, the 300 K equation of state measured for stishovite [zero-pressure bulk modulus K_{0T} = 312.9(±3.4) GPa and pressure derivative K'_0 = 4.8(±0.2) GPa] is inconsistent with the classical interpretation of Hugoniot measurements on quartz and fused silica as representing the properties of stishovite at high pressures. For these materials, shock compression apparently does not achieve the thermodynamically stable, crystalline phase. Recent developments in laser-driven shock experiments [Celliers et al., 2000] allows for measurements to be performed on significantly smaller samples. Therefore the conclusions presented here can be tested directly through laser-driven shock experiments on high-quality, single-crystal stishovite.

References

Ahrens, T. J., D. L. Anderson, and A. E. Ringwood, Equations of state and crystal structures of high-pressure phases of shocked silicates and oxides, *Rev. Geophys.*, 7(4), 667–707, 1969.

Al'tshuler, L. V., R. F. Trunin, and G. V. Simakov, Shock-wave compression of periclase and quartz and the composition of the lower mantle of the earth, *Izv. Akad. Nauk, Ser. Fiz.*, 10, 1–6, 1965.

Andrault, D., C. Fiquet, F. Guyot, and M. Hanfland, Pressure-induced Landau-type transition in stishovite, *Science*, 282, 720–724, 1998.

Birch, F., Finite strain isotherm and velocities for single crystal and polycrystalline NaCl at high pressures and 300 K, *J. Geophys. Res.*, 83, 1257–1268, 1978.

Celliers, P. M., G. W. Collins, L. B. Da Silva, D. M. Gold, R. Cauble, R. J. Wallace, M. E. Foord, and B. A. Hammel, Shock-induced transformation of liquid deuterium into a metallic fluid, *Phys. Rev. Lett.*, 84, 5564–5567, 2000.

Chao, E. C. T., J. J. Fahey, and J. Littler, Stishovite, SiO_2, a very high pressure new mineral from Meteor Crater, Arizona, *J. Geophys. Res.*, 67, 419, 1962.

DeCarli, P. S., and D. J. Milton, Stishovite: Synthesis by shock wave, *Science*, 147, 144–145, 1965.

Dixon, J. E., E. Stolper, and J. R. Delaney, Infrared spectroscopic measurements of CO_2 and H_2O in Juan de Fuca Ridge basaltic glasses, *Earth Planet. Sci. Lett.*, 90, 87–104, 1988.

Funamori, N., R. Jeanloz, N. Miyajima, and K. Fujino, Temperature-dependent mineral assemblages of basalt at lower-mantle conditions, *J. Geophys. Res.*, 105, 26,037–26,043, 2000.

Furnish, M. D., and E. Ito, Experimental measurements of shock properties of stishovite, in *Shock Compression of Condensed Matter—1995*, pp. 93–96, Am. Inst. Phys., Woodbury, N.Y., 1996.

Gratz, A. J., W. J. Nellis, J. M. Christie, W. Brocious, J. Swegle, and P. Cordier, Shock metamorphism of quartz with initial temperatures −170 to +1000 degrees C, *Phys. Chem. Miner.*, 19, 267–288, 1992.

Haines, J., J. M. Léger, F. Gorelli, and M. Hanfland, Crystalline post-quartz phase in silica at high pressure, *Phys. Rev. Lett.*, 87, 155,503, 2001.

Hemley, R. J., A. P. Jephcoat, H. K. Mao, L. C. Ming, and M. H. Manghnani, Pressure-induced amorphization of crystalline silica, *Nature*, 334, 52–54, 1988.

Hemley, R. J., J. Shu, M. A. Carpenter, J. Hu, H. K. Mao, and K. J. Kingma, Strain/order parameter coupling in the ferroelastic transition in dense SiO_2, *Solid State Commun.*, 114, 527–532, 2000.

Holmes, N. C., J. A. Moriarty, G. R. Gathers, and W. J. Nellis, The equation of state of platinum to 660 GPa (6.6 Mbar), *J. Appl. Phys.*, 66, 2962–2967, 1989.

Irifune, T. R., and A. E. Ringwood, Phase transformations in subducted oceanic crust and buoyancy relationships at depths of 600–800 km in the mantle, *Earth Planet. Sci. Lett.*, 117, 101–110, 1993.

Ito, H., K. Kawada, and S. I. Akimoto, Thermal expansion of stishovite, *Phys. Earth Planet. Inter.*, 8, 277–281, 1974.

Jackson, I., and H. Niesler, The elasticity of periclase to 3 GPa and some geophysical implications, in *High Pressure Research in Geophysics*, edited by S. Akimoto and M. H. Manghnani, pp. 93–114, Cent. for Acad. Publ. Japan, Tokyo, 1982.

Kesson, S., J. Fitz Gerald, and J. M. G. Shelley, Mineral chemistry and density of subducted basaltic crust at lower-mantle pressures, *Nature*, 372, 767–769, 1994.

Kieffer, S. W., Shock metamorphism of the Cononino Sandstone at Meteor Crater, Arizona, *J. Geophys. Res.*, 76, 5449–5473, 1971.

Kieffer, S. W., P. P. Phakey, and J. M. Christie, Shock processes in porous quartzite; transmission electron microscope observations and theory, *Contrib. Mineral. Petrol.*, 59, 41–93, 1976.

Kingma, K. J., C. Meade, R. J. Hemley, H. K. Mao, and D. R. Veblen, Microstructural observations of α-quartz amorphization, *Science*, 259, 666–669, 1993.

Knittle, E., and R. Jeanloz, Synthesis and equation of state of (Mg, Fe)SiO_3 perovskite to over 100 gigapascals, *Science*, 235, 668–670, 1987.

Kondo, K., T. J. Ahrens, and A. Sawaoka, Shock-induced radiation spectra of fused quartz., *J. Appl. Phys.*, 54, 4382–4385, 1983.

Kubo, A., and M. Akaogi, Post-garnet transitions in the system $Mg_4Si_4O_{12}$-$Mg_3Al_2Si_3O_{12}$ up to 28 GPa: Phase relations of garnet, ilmenite and perovskite, *Phys. Earth Planet. Inter.*, 121, 85–102, 2000.

Li, B., S. Rigden, and R. Liebermann, Elasticity of stishovite at high pressure, *Phys. Earth Planet. Inter.*, 96, 113–127, 1996.

Liu, L. G., W. A. Bassett, and T. Takahashi, Effect of pressure on the lattice parameters of stishovite, *J. Geophys. Res.*, 79, 1160–1164, 1974.

Liu, L., W. A. Bassett, and J. Sharry, New high-pressure modifications of GeO$_2$ and SiO$_2$, *J. Geophys. Res.*, *83*, 2301–2305, 1978.

Lyzenga, G. A., T. J. Ahrens, and A. C. Mitchell, Shock temperatures of SiO$_2$ and their geophysical implications, *J. Geophys. Res.*, *88*, 2431, 1983.

Mao, H. K., and R. J. Hemley, New windows on the earth's deep interior, in *Ultrahigh-Pressure Mineralogy*, edited by R. J. Hemley, Miner. Soc. Am., Washington, D. C., 1998.

Mao, H. K., P. M. Bell, J. W. Shaner, and D. J. Steinberg, Specific volume measurements of Cu, Mo, Pd, and Ag and calibration of the ruby R$_1$ fluorescence pressure gauge from 0.06 to 1 Mbar, *J. Appl.Phys.*, *49*, 3276–3283, 1978.

Mao, H. K., P. M. Bell, K. J. Dunn, R. M. Chrenko, and R. C. DeVries, Absolute pressure measurements and analysis of diamonds subjected to maximum static pressures of 1.3–1.7 Mbar, *Rev. Sci. Instrum.*, *50*, 1002–1009, 1979.

Mao, H. K., R. J. Hemley, Y. Fei, J. F. Shu, L. C. Chen, A. P. Jephcoat, Y. Wu, and W. A. Bassett, Effect of pressure, temperature, and composition on lattice parameters and density of (Fe, Mg)SiO$_3$-perovskites to 30 GPa, *J. Geophys. Res.*, *96*, 8069–8079, 1991.

Marsh, S. P., *LASL Shock Hugoniot Data*, Univ. of Calif. Press, Berkeley, 1980.

McQueen, R. G., J. N. Fritz, and S. P. Marsh, On the equation of state of stishovite, *J. Geophys. Res.*, *68*, 2319–2322, 1963.

Ng, A., B. K. Godwal, J. Waterman, L. DaSilva, N. W. Ashcroft, and R. Jeanloz, Nonequilibrium shock behavior in quartz, *Phys. Rev. B*, *44*, 4872–4876, 1991.

Olinger, B., The compression of stishovite, *J. Geophys. Res.*, *81*, 5341–5343, 1976.

O'Neill, B., and R. Jeanloz, MgSiO$_3$-FeSiO$_3$-Al$_2$O$_3$ in the Earth's lower mantle: Perovskite and garnet at 1200 km depth, *J. Geophys. Res.*, *99*, 19,901–19,915, 1994.

Podurets, M. A., G. V. Simakov, and G. S. Telegin, On the phase equilibrium in shock-compressed quartz and on the kinetics of phase transitions, *Izv. Earth Phys.*, *7*, 3–11, 1976.

Podurets, M. A., G. V. Simakov, G. S. Telegin, and R. F. Trunin, Polymorphism of silica in shock waves and equation of state of coesite and stishovite, *Izv. Earth Phys.*, *17*, 9–15, 1981.

Robie, R. A., *Thermodynamic Properties of Minerals and Related Substances at 298.15 K and One Atmosphere*, U.S. Govt. Print. Off., Washington, D. C., 1968.

Ross, N. L., J. F. Shu, R. M. Hazen, and T. Gasparik, High-pressure crystal chemistry of stishovite, *Am. Mineral.*, *75*, 739–741, 1990.

Sato, Y., Pressure-volume relationship of stishovite under hydrostatic compression, *Earth Planet. Sci. Lett.*, *34*, 307–312, 1977a.

Sato, Y., Equation of state of mantle minerals determined through high-pressure X-ray study, in *High Pressure Research: Applications in Geophysics*, edited by M. H. Manghnani and S. Akimoto, pp. 307–324, Academic, San Diego, Calif., 1977b.

Schneider, H., and J. R. Ashworth, Deformation and transformation in experimentally shock-loaded quartz, *Phys. Chem. Miner.*, *11*, 241–249, 1985.

Sharp, T. G., A. El Goresy, B. Wopenka, and M. Chen, A post-stishovite SiO/sub 2/polymorph in the meteorite Shergotty: implications for impact events, *Science*, *284*, 1511–1513, 1999.

Stishov, S. M., Rutile-like silica and phase transformations in the Earth's interior, *Tectonophysics*, *1*, 223–226, 1964.

Stöffler, D., and U. Hornemann, Quartz and feldspar glasses produced by natural and experimental shock, *Meteoritics*, *7*, 371–394, 1972.

Sugiyama, M., S. Endo, and K. Koto, The crystal structure of stishovite under pressure up to 6 GPa, *Mineral. J.*, *13*, 455–466, 1987.

Swamy, V., S. K. Saxena, B. Sundman, and J. Zhang, A thermodynamic assessment of silica phase diagram, *J. Geophys. Res.*, *99*, 11,787–11,794, 1994.

Tsuchida, Y., and T. Yagi, A new, post-stishovite high-pressure polymorph of silica, *Nature*, *340*, 217–220, 1989.

Wackerle, J., Shock-wave compression of quartz, *J. Appl. Phys.*, *33*, 922, 1962.

Wanatabe, W., Thermochemical properties of synthetic high-pressure compounds relevant to the Earth's mantle, *High-Pressure Research in Geophysics*, edited by S. Akimoto and M. H. Manghnani, Cent. for Acad. Publ., Tokyo, 1982.

Weidner, D. J., J. D. Bass, A. E. Ringwood, and W. Sinclair, The single-crystal elastic moduli of stishovite, *J. Geophys. Res.*, *87*, 4740–4746, 1982.

Williams, Q., R. J. Hemley, M. B. Kruger, and R. Jeanloz, High-pressure infrared spectra of alpha-quartz, coesite, stishovite and silica glass, *J. Geophys. Res.*, *98*, 22,157–22,170, 1993.

Zhang, J., and D. J. Weidner, Thermal equation of state of aluminum-enriched silicate perovskite, *Science*, *284*, 782–784, 1999.

———————————

L. R. Benedetti, Department of Physics, University of California, Berkeley, CA 94720, USA.

R. Jeanloz, Department of Earth and Planetary Science, University of California, Berkeley, CA 94720, USA.

W. R. Panero, Department of Geological Sciences, University of Michigan, 2534 CC Little Building, 425 E. University, Ann Arbor, MI 48109-1063, USA. (wpanero@umich.edu)